Investigation of Limb-Side Stick Dynamic Interaction with Roll Control

Donald E. Johnston* and Duane T. McRuer†
Systems Technology, Inc., Hawthorne, California

A fixed-base simulation was performed to identify and quantify interactions between the pilot's hand/arm neuromuscular subsystem and such features of modern fighter aircraft roll-rate command control system mechanizations as force-sensing side-stick-type manipulator, vehicle effective roll time constant, and flight control system effective time delay. The results provide insight to high-frequency pilot/vehicle oscillation (roll ratchet), low-frequency pilot-induced oscillation, and roll-to-right control input problems previously observed in experimental and production fly-by-wire control systems. The simulation configurations encompass and/or duplicate several actual flight situations, reproduce control problems observed, and show that the high-frequency nuisance mode known as "roll ratchet" can derive primarily from the pilot's neuromuscular subsystem. The simulations show that force-sensing side-stick manipulator force/displacement/command gradients, command prefilters, and flight control system time delays need to be carefully adjusted to minimize neuromuscular mode amplitude peaking (roll-ratchet tendency) without restricting roll control bandwidth (with resulting sluggish or low-frequency pilot-induced oscillation prone control). The results further demonstrate that roll-ratchet tendency, difficult to detect in fixed-base simulations, is readily apparent from application of frequency-response spectral analysis techniques.

Introduction

ALMOST every new aircraft with fly-by-wire or command augmentation (Fig. 1) in the roll axis has encountered either pilot-induced oscillations (PIO) or roll ratcheting (or both) in early flight phases. PIO has typically been associated with high-gain, neutrally stable, closed-loop pilot-vehicle control oscillations with a frequency of about ½ Hz. The "roll ratchet" has been somewhat more obscure and idiosyncratic, appearing most often in rapid rolling maneuvers. Ratchet frequencies are typically 2–3 Hz. Figure 2[1] illustrates this often remarked but seldom recorded phenomenon. The frequency difference alone indicates that the PIO and ratchet situations are different phenomena, yet both clearly involve the closed-loop pilot vehicle system.

An interesting set of roll-ratcheting phenomena has been observed in variable stability NT-33 flight.[2-4] Chalk[5] speculates that the oscillations were due to the near K_c/s character of the effective controlled element. He used a rudimentary ($K_p e^{-\tau s}$) nonadaptive pilot model with τ ranging from 0.09 to 0.13 s to show that one can get the observed instability (at about 12–17 rad/s) with a K/s-like aircraft and high pilot gains. This effective time delay must account for *all* the open-loop system lags, i.e., controller, actuator, filters, etc., plus the effective latency of the pilot. So, if this explanation of the roll ratchet is to be reasonable, the total τ value must be appropriate. The 0.09–0.13 s range is remarkably low for the pilot alone and is very low indeed when aircraft plus control system effective lags are also considered.

Mitchell and Hoh[6] also examined some of the same data. They cite sinusoidal vibration data in which a simple lateral tracking task was performed (using a center stick) while under the influence of high-frequency lateral accelerations.[7] Frequencies from 1 to 10 Hz were employed, and an oscillatory arm/stick "bobweight" mode occurred at about 12 rad/s. Mitchell and Hoh note that this higher-frequency mode of the pilot-aircraft systems is near the frequencies of the observed ratcheting in F-16 and Calspan flight experiments, and they cite it as a possible cause.

From the earliest studies on the interaction between the human pilot's neuromuscular system and aircraft control devices,[8,9] the presence of a neuromuscular system limb-manipulator dynamic resonance peak at 14–19 rad/s has been well known. Neuromuscular system characteristics are cited[10] as "exceptionally important and critically limiting in such matters as: control precision (where limited by the pilot's neuromuscular system dynamics) and effects of control system nonlinearities (including their connections with control system sensitivity requirements)." Other summaries[11] place great stress on the importance of considering these characteristics, even though this frequency range of major activity may be well above the bandwidth associated with the "usual" control task.

It is becoming more and more apparent that modern high-performance high-gain command-response flight control system bandwidths may be encroaching on the neuromuscular system. Advances in flight control system fly-by-wire technology permit new manipulation devices, for example, force-sensing side sticks, at the pilot output/effective vehicle interface. These have thus far been generally successful in application but have introduced or enlarged some pilot-vehicle flying qualities problems. Particular problems include[2-4,12,13]

1) High roll control sensitivity and PIO's in precision maneuvering.

2) Roll ratchet in otherwise steady rolling maneuvers.

3) Sensitivity to the way the pilot grips the stick or to location of his hand/arm support.

4) Effective time delay associated with stick filters with attendant increase in pilot remnant.

5) Biodynamic interactions, e.g., hand/arm stick bobweight effects.

Attempts to alleviate these effects have involved adjustments in stick force gradients, filtering, and sensitivity. These have included introduction of various nonlinear elements, such as command gain reduction as a function of

Received July 9, 1985; presented as Paper 85-1853 at the AIAA Guidance, Navigation, and Control Conference, Snowmass, CO, Aug. 19–21, 1985; revision received June 5, 1986.

*Principal Research Engineer, Associate Fellow. AIAA.
†President and Technical Director. Fellow AIAA.

pilot input amplitude or frequency, filter time constant changes with sense of input (increase vs decrease), and different force gradient for right and left roll commands. These adjustments have generally involved ad hoc empirical modifications in the course of the aircraft development. Much of this has been accomplished in flight tests with a correspondingly large cost.

The purposes of this paper are to

1) Explore the origins of the roll-ratchet phenomenon.

2) Develop insights about the tradeoffs involved in adjusting the properties of force-sensing side sticks.

3) Present guidelines to minimize roll control problems.

Human Pilot Dynamic System Considerations

Ideal Crossover Model (and Its Implications)

The prescription for K/s-like controlled element dynamics in the region of pilot-vehicle system crossover as an often desirable form stems from the fundamental feature of human dynamics that no pilot lead is then required to establish good closed-loop system dynamics over a wide range of pilot gains. The basic recipe is almost invariably conditioned by such statements as "in the frequency region about crossover." Such statements are made to restrict the form of the pilot model to that required *only* in the crossover region. In particular, the cases covered are such that an effective time-delay term in the pilot model is an adequate approximation to the high-frequency effects.

Simple tracking task pilot model forms and associated pilot-vehicle system properties begin with the ideal crossover model[11] of Fig. 3. In this model, the pilot adjusts his dynamic characteristics so that the amplitude ratio of the open-loop pilot-vehicle dynamics approximate $|\omega_c/j\omega|$ over the frequency band immediately above and below the gain crossover. The model also indicates that in full-attention tracking operations, the pilot will adjust his gain to offset any variation in controlled element gain in order to maintain a nearly fixed control system bandwidth. Thus, the full-attention closed-loop bandwidth ω_c (identified as the crossover of the 0-dB gain line with the K/s-amplitude ratio plot) is independent of the controlled element gain.

In the crossover model, the exponential term with time delay τ approximates all the lag contributions due to pilot and vehicle high-frequency dynamic modes. The effective time delay is a function of, among other things, the force/displacement characteristics of the manipulator. As shown in Fig. 3, an isometric (force) stick results in less lag than an isotonic (free-moving) stick does. Past experimentation[14] has identified the difference as approximately 0.1 s.

In Fig. 3, if the pilot gain were set at the value represented by K_{p_2} with an isometric stick, the bandwidth would be indicated by ω_{c_2} and would result in a system stability phase margin ϕ_{m_2}, and gain margin GM. If this same gain were employed with the isotonic stick, the phase margin would be 0, and a low-frequency continuous oscillation (PIO) would result. This oscillation can then be alleviated by pilot gain reduction to the value represented by K_{p_1}; thereby, accepting a reduced bandwidth. Thus, Fig. 3 can be used to demonstrate the common low-frequency PIO problem that generally occurs in the vicinity of 0.5 Hz and that is relieved by reducing pilot gain. (In the crossover model, an ω_u of 4 rad/s corresponds to $\tau = \pi/2\omega_u \doteq 0.4$ s for the total pilot, control system, aircraft, etc., latency.)

Limb-Side Stick Neuromuscular Model (and Its Implications)

As previously cited, early studies on the neuromuscular system noted the presence of a neuromuscular system or limb-manipulator (NM/L) peak at 14–19 rad/s well past the usual "crossover region."[8] The effects of various restraints on the limb/neuromuscular system have been identified via closed-loop neuromuscular system model fits to pilot/controlled-element describing function measurements for pressure and free-moving manipulators.[9] An important part of the neuromuscular dynamics in each case is a quadratic mode with damping ratio and undamped natural frequency $[\zeta, \omega_n]$ of:

Manipulator:	NM/L dynamics:
Free-moving	[0.07, 17]
Isometric or pressure	[0.138, 18.6]

There is also a neuromuscular system mode that is approximated by a first-order lag break at about 10 rad/s. This

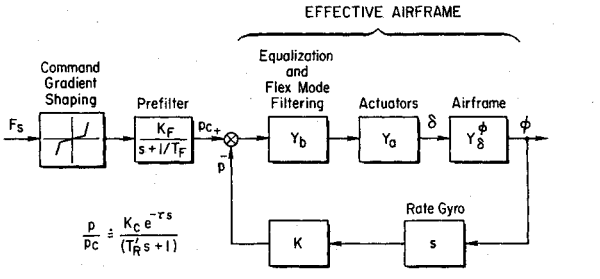

Fig. 1 Typical fly-by-wire roll control system.

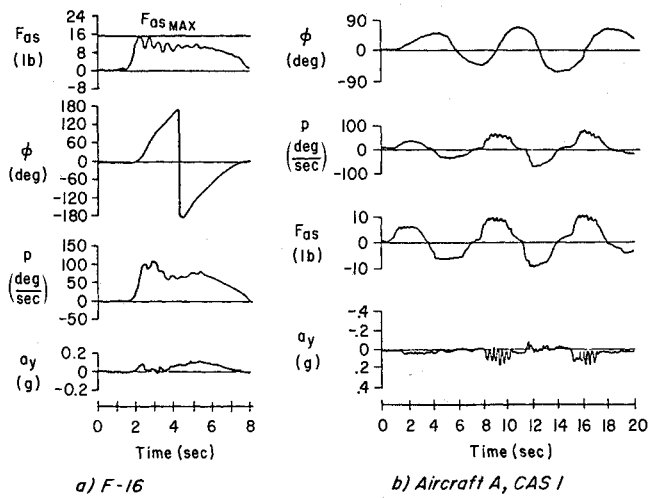

Fig. 2 Roll ratchet during banking maneuver.[1]

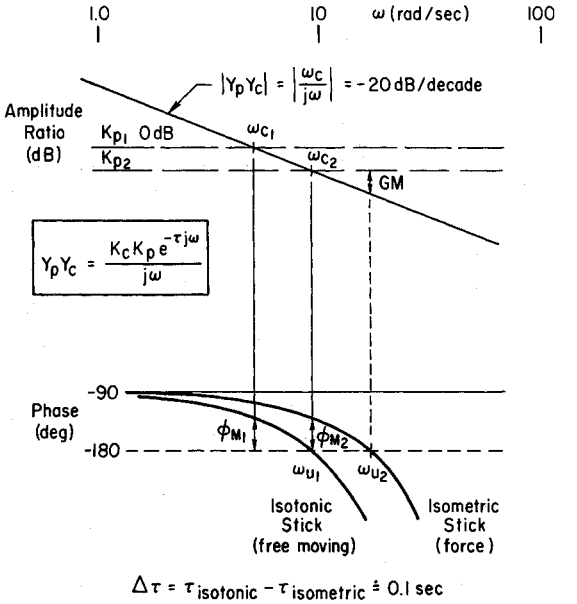

$\Delta\tau = \tau_{isotonic} - \tau_{isometric} \doteq 0.1$ sec

Fig. 3 Ideal crossover model.

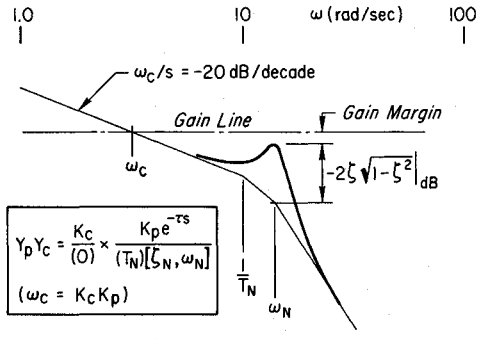

Fig. 4 Bode amplitude plot for neuromuscular system contribution to roll ratchet potential.

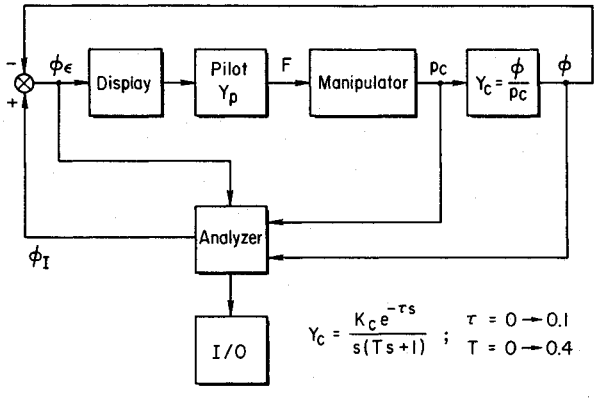

Fig. 5 Experimental setup.

mode is also somewhat dependent on the nature of the manipulator restraints.[14,15]

The reason the neuromuscular actuation system dynamics differ when the manipulator restraints are changed is physiological—the neuromuscular apparatus involved depends on the restraints and limb movements. While greatly oversimplified, the neuromuscular actuation elements of the human may be viewed as a two-loop system. The inner loop principally involves Golgi, muscle spindle, and other receptors with short pathways directly to spinal level and back to the musculature. Viewed from the output end, this loop is primarily sensitive to forces and, because of the short neural pathways, the time lags of information flow are small. The effective bandwidth of this loop can therefore be quite high. The second or outer loop includes joint and other (e.g., peripheral vision) receptors as major feedback elements. Their neural pathways and associated delays are longer leading to a lower outer-loop bandwidth. In isometric (force-stick) manipulator conditions, there is little or no joint movement, so the inner-loop elements should be dominant. With isotonic (free-moving stick) conditions, on the other hand, the joint receptors also enter as major elements. As already indicated in connection with Fig. 3, the net difference in terms of an effective latency is approximated at low frequencies by a difference in effective τ of about 0.1 s.

If we now employ the detailed model of the neuromuscular system (instead of only approximating its phase lag contribution as in Fig. 3) and superimpose it on the controlled element K/s as in Fig. 4, we see an open-loop resonant peak in the 2-3 Hz frequency range due to the neuromuscular system. The correspondence of the neuromuscular/limb quadratic mode numerical values and observed roll-ratchet frequencies is very unlikely to be a coincidence. So at observed roll-ratchet frequencies, the neuromuscular/limb mode should clearly be taken into account. Since their primary effect is a resonant peak from which a "gain margin" might be measured,‡ these properties may be of central importance for high-gain pilot situations.

Experiment Goals and Setup

The experimental goals were to investigate and quantify limb/manipulator dynamics and interactions between the neuromuscular subsystem, force-sensing side-stick configuration, high-gain command augmentation, and command filtering, and to investigate possible relationships between these interactions and the roll-ratchet phenomenon. A longer-range goal is to provide and enhance guidelines for manipulator-system design.

The experimental setup is depicted in Fig. 5. A roll tracking task was selected in which the pilot matches the bank angle of his controlled element with that of a "target" having pseudo random rolling motions Φ_I. The random motions are obtained via a computer-generated sum of sine waves, Table 1. The error is displayed on a CRT, and the pilot attempts to null the error by applying force to the manipulator, the output of which becomes the command to the controlled element Y_c. The form of the controlled element is identified in Fig. 5, along with the range of lag-time constants and time delays utilized in the experiment. This controlled element approximates a high-gain roll-rate command system. The time-lag parameter T may be considered to be the effective roll subsidence time constant or a flight control system prefilter (between the pilot's stick command and the flight control system), whichever is larger. For very small values of τ, the pure time delay may be a realistic approximation to digital flight control system sample and hold dynamics. More generally, it is a low-frequency approximation for all the high-frequency lags in the system that are not covered by the time lag T. Because we are interested primarily in modern flight control systems, the parameter values for T and τ used in the experiment are generally consistent with values that would be present in a system designed to be Level 1 on the basis of flying-qualities specifications. Thus, the parameter values used generally should produce excellent effective controlled elements, providing the gain is appropriately adjusted.

The manipulator was a McFadden Systems, Inc., center-stick and force loader system used in many aircraft research and development simulations. The subject was seated to the left of the stick and provided with an adjustable armrest to produce an effective side-stick configuration for all runs. Three stick displacement configurations were employed. One was a fixed (no displacement) stick as in the F-16A.[12] The second had 0.77-deg/lb (small) motion/force gradient. The third had 1.43-deg/lb (large) stick motion/force gradient. The latter two matched the displacement/force characteristics employed in an NT-33 flight test.[13] In all cases, the stick displacements necessary to generate the required force signal did not entail *arm* movement. Analog signals from the manipulator force sensor p_c and the resulting controlled element roll response ϕ were passed through an analog-to-digital converter to a digital computer where Y_pY_c describing functions and various performance measures were computed using STI's Frequency Domain Analysis (FREDA) program. The computations were essentially on-line and printed out at the conclusion of each run. Some 530 data runs were accomplished with two highly trained subjects, which provided a large data base from

‡While the "gain margin" shown in Fig. 4 indicates the magnitude difference between the $|Y_pY_c|_{dB}$ peak and the 0=dB line, the phase at or near this frequency may differ appreciably from that required for instability. Thus, when the "gain margin" shown is zero only one of the two conditions for instability may be satisfied. Consequently, this is not necessarily a true gain margin in the conventional sense. It does, however, indicate a resonant tendency contributed by the pilot.

Table 1 Roll tracking forcing function[a]

Sine wave (i)	1	2	3	4	5	6	7	8	9
Frequency (ω_i)	0.467	0.701	1.17	1.87	3.51	7.01	11.2	14.0	18.7
Amplitude (A_i)	15.2	15.2	15.2	7.6	3.04	0.76	0.38	0.228	0.152
Relative amplitude	1	1	1	0.5	0.2	0.05	0.025	0.015	0.01

[a] $\phi_1 = \Sigma A_i \cos\omega_i t$(deg)

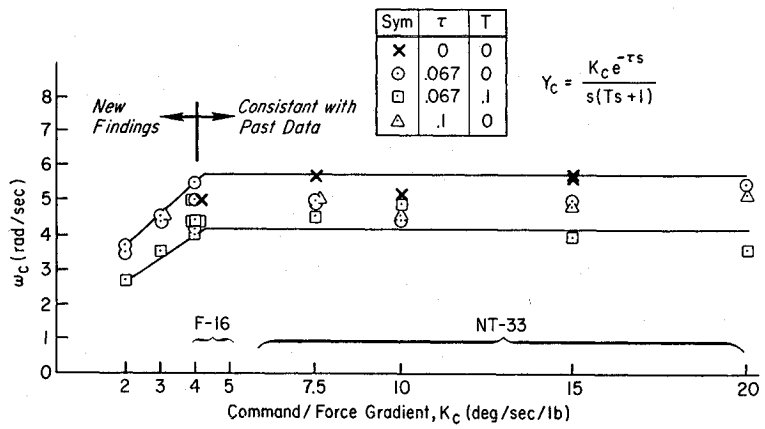

Fig. 6 Influence of command/force gradient on crossover (fixed stick).

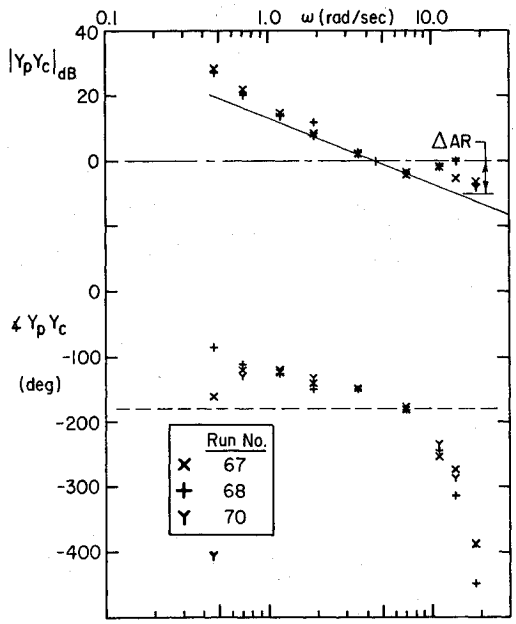

Fig. 7 Y_pY_c describing function amplitude and phase plot for $Y_c = 4/se^{-0.067s}$.

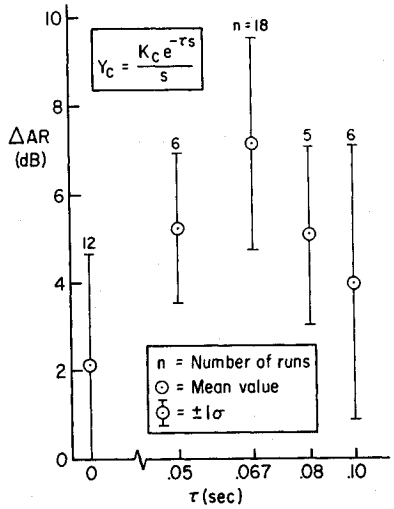

Fig. 8 Neuromuscular system amplitude ratio peaking with controlled element time delay (fixed stick).

which to determine or identify the various interactions of interest.

No accounts have been found where roll ratchet has been observed or recognized in fixed- or moving-base simulations. Apparently it has occurred only in actual flight, and then on a more or less random basis. The first objective of this experimental setup, therefore, was to tune the controlled element, manipulator, and command/force gradients to try to achieve roll ratchet, or at least maximize roll-ratchet tendencies in the fixed-base simulation. A key factor was that describing function measurements must cover the limb neuromuscular peaking frequency region, and the forcing function (Table 1) was adjusted to emphasize good data in the neuromuscular subsystem region. Further, the open-loop system describing function Y_pY_c was selected for examination because it would emphasize any peaking tendencies present and could also be adjusted to account for the first-order effects of aircraft motions on these fixed-base data.

Experimental Results

Human Pilot Dynamics

It will be recalled that in the ideal crossover model, the crossover frequency remains constant even though the controlled element gain may vary. Figure 6 shows results obtained using the fixed side-stick manipulator configuration and a wide range of command/force gradients (controlled element gains). The ranges of command/force gradients for the F-16[12] and the NT-33[13] experimental flight programs are identified for comparison. The controlled element forms range from K/s to $Ke^{-0.067s}/s(0.1s+1)$. The data points for various time delay

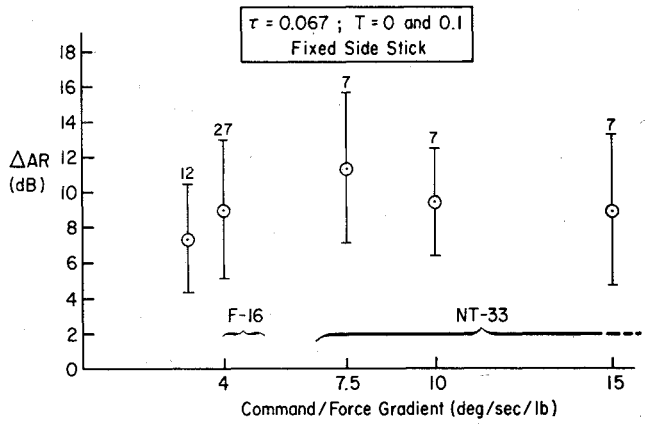

Fig. 9 Neuromuscular peaking sensitivity to controlled element command/force gradient.

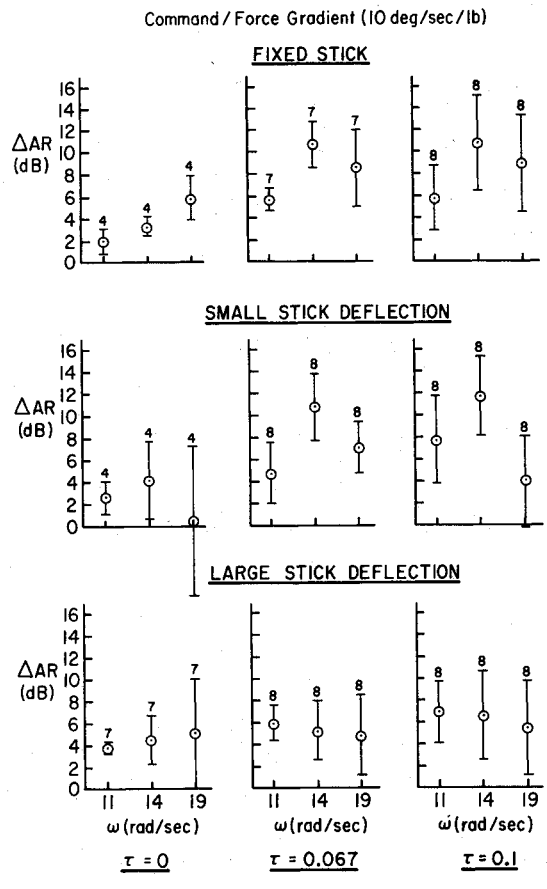

Fig. 10 Influence of stick displacement on neuromuscular peaking tendency.

or time lags are indicated by the symbols. The data of Fig. 6 indicate two aspects. First, they reflect a general decrease in ω_c as controlled element lags increase. Second, they show that crossover frequency, as expected, is essentially independent of controlled element gain over a very broad region. But, as the controlled element gain becomes quite low and the manipulator forces required to achieve the desired rolling response become very large, a point is reached where the pilot can no longer accommodate, and a rapid dropoff in pilot-vehicle system bandwidth results. Interestingly, the F-16 initial command/force gradients lie right at the break in ω_c, and therefore represent the lowest values that might be considered acceptable to pilots.

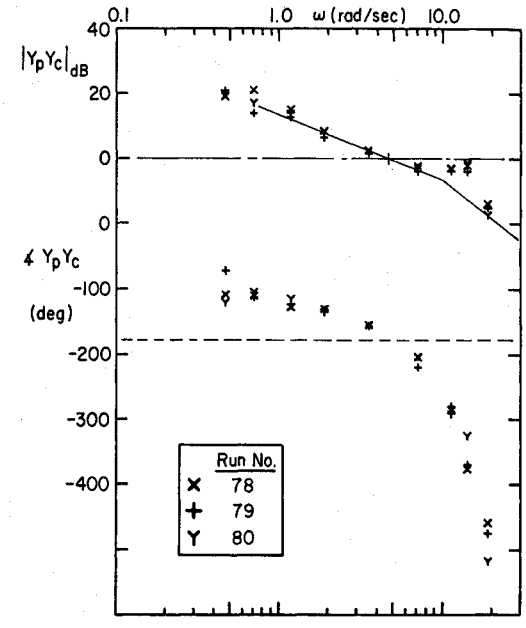

Fig. 11 Y_pY_c describing function amplitude and phase plot for $Y_c = [4e^{-0.067s}/s(0.1s+1)]$.

Similar results were obtained with the small and large displacement side-stick configurations, except that the crossover frequencies decreased slightly as the displacement was increased.

Neuromuscular System Peaking Tendencies

We now turn our attention to the neuromuscular system. Figure 7 presents the describing function measurements for three runs using the fixed force stick, and a controlled element having a command/force gradient of 4 deg/s/lb, no time lag, and a time delay of about 67 ms. The straight line reflects the resulting ω_c/s crossover characteristics. Amplitude departures from this asymptote are the contributions of the pilot's neuromuscular system at high frequency and his trim lag-lead at low frequency. In the region of crossover, Y_pY_c is almost exactly ω_c/s, as suggested by the ideal crossover model. The amplitude ratio departures from the asymptote at the highest three frequencies shows a peaking in the vicinity of the 14 rad/s forcing function for two of the three runs. It also might be noted that there is remarkable consistency in both the amplitude and phase measurements across all frequencies for all three runs. In Fig. 7, two of the amplitude data points at 14 rad/s lie slightly above the 0-dB line. We would, therefore, expect this to represent a neutral or slightly unstable dynamic mode if the phase angle were near -180 deg at this frequency. This then could be interpreted as affecting roll ratchet. More will be said about this later.

The two data points at 14 rad/s are 10 dB above the asymptote and may or may not be exactly the actual neuromuscular system peak; i.e., the peak itself may occur at a slightly higher or lower frequency. The peaking tendency shown in Fig. 7 is representative of a large amount of the data obtained. This frequency is consistent with the roll-ratchet frequencies observed in the flight traces.

Influence of Effective Controlled Element Characteristics

The sensitivity of the 14-rad/s peaking tendency to time delay is shown in Fig. 8. The circles reflect the average values at each frequency, and the bars indicate $\pm 1\ \sigma$ ranges. The controlled element is $K_ce^{-\tau s}/s$. The manipulator is the fixed-stick configuration. Results show that a time delay in the vicinity of 0.067 s tends to maximize the neuromuscular

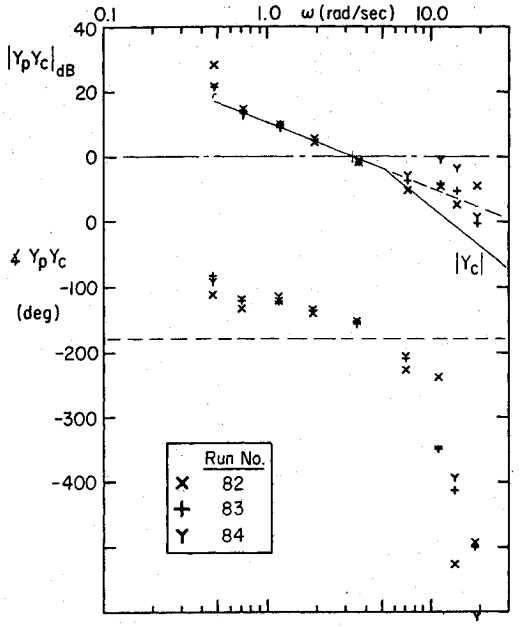

Fig. 12 Y_pY_c describing function amplitude and phase plot for $Y_c = [4e^{-0.067s}/s(0.2s+1)]$.

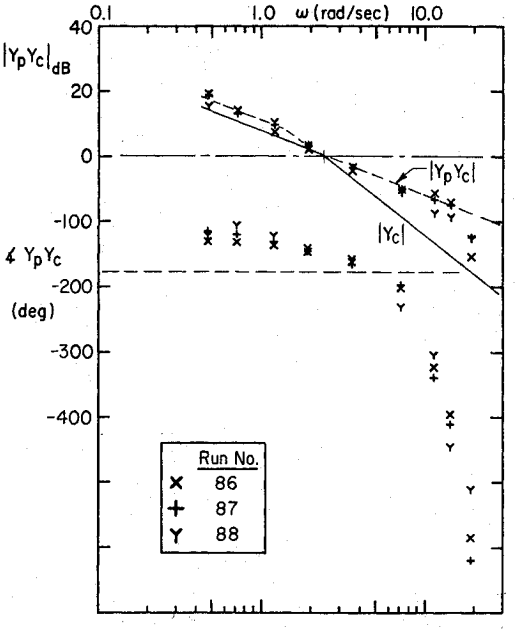

Fig. 13 Y_pY_c describing function amplitude and phase plot for $Y_c = [4e^{-0.067s}/s(0.4s+1)]$.

system peaking. At time delays either below or above these values, the peaking tendency decreases. Of all the controlled elements examined, K_c/s shows the minimum tendency for a peak. Interestingly, the time delay values that maximize the neuromuscular peaking would be considered good from the MIL-8785 flying quality specification standpoint. In essence, these data show that the tendency to peaking can be "tuned" by the adjustment of the controlled element effective lag with a maximum effect near 0.07 s.

The neuromuscular system peaking sensitivity to controlled element command/force gradient is shown in Fig. 9. Here the command/force gradient ranges from 3 deg/s/lb (which is slightly lower than that employed on the F-16) up through 15 deg/s/lb, which was utilized in the NT-33. The data were obtained using the fixed stick and a time delay of

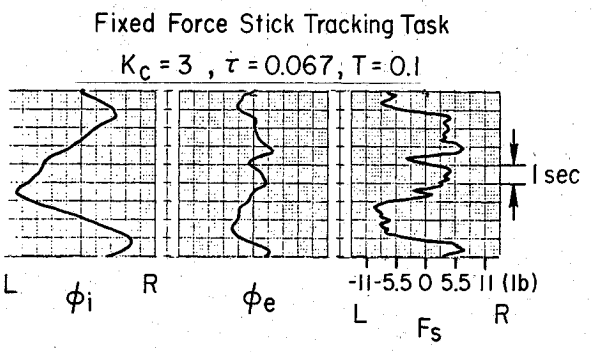

Fig. 14 Example of rollratchet-like oscillation in stick force trace.

0.067 s. Data for time lags of 0 and 0.1 have been combined. These data show a slight increase in peaking tendency in the vicinity of 7.5-deg/s/lb command/force gradient. This is about the same value as the response/force ratio for the Fig. 2 flight traces of ratchet. This may or may not be coincidental. However, it is significant that there is appreciable peaking of the neuromuscular system across the entire gain range investigated in these experiments.

Influence of Stick Characteristics

The influence of stick motion is summarized in Fig. 10. These plots reflect the amplitude ratio peaking at the three higher frequencies (11, 14, and 19 rad/s) for the fixed, the small-deflection, and the large-deflection stick configurations at three different values of the controlled element time delay: 0.0, 0.067, and 0.1 s. All these data were taken with the command/force gradient of 10 deg/s/lb. The results show that there is relatively little difference between the fixed and small-deflection force stick. Both show an increase in neuromuscular peaking tendency for the 0.067- and 0.1-s time delays. They both show a tendency to maximum peaking in the vicinity of 14 rad/s and, in both cases, there is considerably less peaking for the zero time-delay cases. The large-deflection stick, on the other hand, shows a relatively constant amplitude departure from the controlled element asymptote across the 11-19-rad/s frequency band and a lack of sensitivity to the controlled element time delay.

Adjustment of Pilot Lead

The influence of the lag time constant on the neuromuscular system peaking, aks well as the possible adoption of lead by the pilot, is reflected in Figs. 7 and 11-13. Figure 7 shows the neuromuscular peaking obtained with the controlled element command/force gradient of 4 deg/s/lb, a time delay of 0.067 s, and no lag. The maximum peaking was noted to be approximately 10 dB and occurred at 14 rad/s. The addition of a first-order lag-time constant of 0.1 s is shown in Fig. 11. Here the solid line represents the controlled element Y_c Bode asymptote adjusted to go through ω_c. The crossover occurs in a region that is K/s in appearance, and the amplitude peaking again is approximately 10 dB and occurs near the 14-rad/s data point. The peaks are quite close to the 0-dB gain line, so this amplitude ratio feature satisfies one of the two conditions for a closed-loop neutral stability, and thus a possible tendency to roll ratchet. Comparison of the phase plots between Figs. 7 and 11 indicate that the pilot is generating little if any lead to offset the time lag. (Detailed analyses[16] indicate that there is a pilot lead near 8 rad/s for these cases, and for $Y_c = K/s$, which tends to compensate for the high-frequency lags in general but cancels none of them.)

In Fig. 12, the time lag has been moved to 0.2 s. Comparison of the phase angle data points in Figs. 7 and 12 or Figs. 11 and 12 indicates that the pilot has introduced lead in

the Fig. 12 case, which essentially cancels the time lag at 0.2 s. The asymptote for the Y_p/Y_c open-loop system is thus represented by the solid line at frequencies below the time constant break point and the dashed line above that break point. Again, the amplitude ratio is ω_c/s-like in the vicinity of the crossover. However, there is now considerable scatter in the data points in the region of the neuromuscular system peaking dynamics. In only one of the three runs shown in Fig. 12 was there a peaking tendency for the neuromuscular system, and this appears to be in the vicinity of 11 rad/s rather than the 14 noted previously. In the other two runs, the amplitude data points lie quite close to the Y_pY_c asymptote.

In Fig. 13, the lag-time constant has been moved down to 0.4 s. Again, comparison of the phase plots shows that the pilot has now moved his lead down to precisely cancel the controlled element time-lag contribution so that the resulting Y_pY_c has the appearance of an ω_c/s throughout the frequency region of interest. The peaking tendency of the neuromuscular system is no longer evident, and there should be little chance of roll ratchet. However, the roll control bandwidth has now been reduced to approximately 2.5 rad/s, whereas it was approximately 4.5 rad/s with the time constant of 0.1 s. If the pilot were to attempt to achieve a 4.5-rad/s bandwidth in the presence of the lag characteristics shown in Fig. 13, a PIO would occur at roughly that frequency (4 rad/s). Thus, in reducing or eliminating the roll-ratchet tendency, we may have substituted a tendency for the lower-frequency PIO.

Closed-Loop Pilot-Vehicle System Characteristics

Observed Fixed-Base Roll Ratchet

The previous sections have emphasized the neuromuscular peaking tendency as a harbinger of the roll ratchet phenomenon. Yet in the data presented, the open-loop system phase angle has generally been greater in magnitude than -180 deg. This means that the gain differences between the peak and the O-dB line are not necessarily true gain margins. The closed-loop pilot-vehicle systems will therefore not necessarily show an oscillation at the neuromuscular peaking frequency, although a resonant peak somewhat reduced from the open-loop peak will often be indicated in the closed-loop system. The pilot remnant being relatively broadband in character, will therefore act as a driving mechanism to excite the resonant peak.

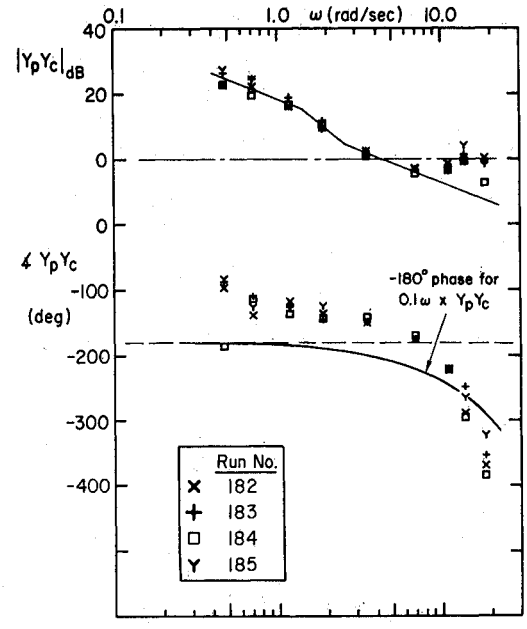

Fig. 15 Expected phase shift due to motion effects.

In some cases, the experimental data actually indicated a rollrachet-like oscillation under conditions similar to those where the phenomenon was found in flight. Most commonly these were stretches in the time histories that involved nearly steady-state rolling velocity commands. An example is given in Fig. 14. Here, a short segment of the roll attitude command input is nearly triangular, and the pilot's stick force trace indicates a 2-3-Hz oscillation. Because the forcing function is a random-appearing time signal with only very occasional segments akin to the triangular or steady rolling commands shown, this type of ratchet-like pilot output trace is atypical in the context of a total experimental run. The pilot subjects, in fact, did not report that they had encountered the condition since it was so transitory. Yet it appeared quite commonly once the conditions were favorable—i.e., neuromuscular peaking tendency present and momentarily steady rolling velocity command. Consequently, the fixed-base simulation can be said to have successfully demonstrated rollratchet-like phenomena.

It is particularly enlightening and useful to reexamine the open-loop describing function data when a first-order adjustment is made to the phase data to account for the effect of rapid rolling motion on the pilot during flight. The pilot's angular-motion-sensing neurological apparatus acts very much like a rate gyro inner loop in the frequency range near and slightly above crossover.[11] This inner loop, present when rolling velocities exceed the pilot's neurological threshold, has the effect of reducing the effective time lags in the pilot's visual-input/manipulator-output response. The reduction can be as much as 0.1 s from the fixed-base data.[17,18] When changes of phase lag of the magnitude 0.1 ω rad are made on typical describing function data showing major neuromuscular peaking, the net phase shift in the frequency region about the peak is very often near -180 deg. Figure 15 shows a typical example for the fixed force stick configuration with $T=0$, $\tau=0.067$, and $K_c=10$ deg/s/lb. Therefore, one can conclude that the fixed-base neuromuscular peaking examples, which show negative gain margins of the amplitude ratio peak relative to 0 dB, are quite likely to result in oscillations in the "moving-base" flight situation. The roll ratchet phenomenon in these cases would, therefore, be high-frequency PIO's, which intimately involve the pilot's limb-manipulator neuromuscular system dynamics.

Comparisons with Flight Data

The controlled elements in Figs. 11-15 essentially duplicate the F-16 configurations tested,[12] and the qualitative results and trends are the same. The compromise selection for the prefilter in the F-16 was a time constant of 0.2 rad/s, which is shown in Fig. 12 to allow a comfortable bandwidth slightly above 3 rad/s, and having 30-35-deg of phase margin and a much reduced neuromuscular peaking tendency. Thus, there should be minimum tendency for either low- or high-frequency PIO, although the data scatter in the higher-frequency range of Fig. 12 shows that conditions favorable to roll ratchet could pop up from time to time.

Yet another comparison between simulation results and flight data can be drawn from the investigation of roll ratchet and various prefilter configurations flown in the NT-33.[3] In this case, one set of effective controlled elements are a close match to this simulation. A major difference, however, was the use of a center stick in the NT-33. The roll ratchet encountered in this flight test was described as "response which was objectionably abrupt, resulting in a very high frequency pilot-induced-oscillation (wing rocking), or having 'square corners' or being very 'jerky.' " The frequency was approximately 16 rad/s.

Figure 16 is a replot of data from Ref. 3 with command/force gradient plotted vs the roll time constant T_R. The circles identify configurations flown; the open symbols reflect no ratchet obtained, the shaded symbols reflect roll ratchet observed by one or more of the evaluation pilots over

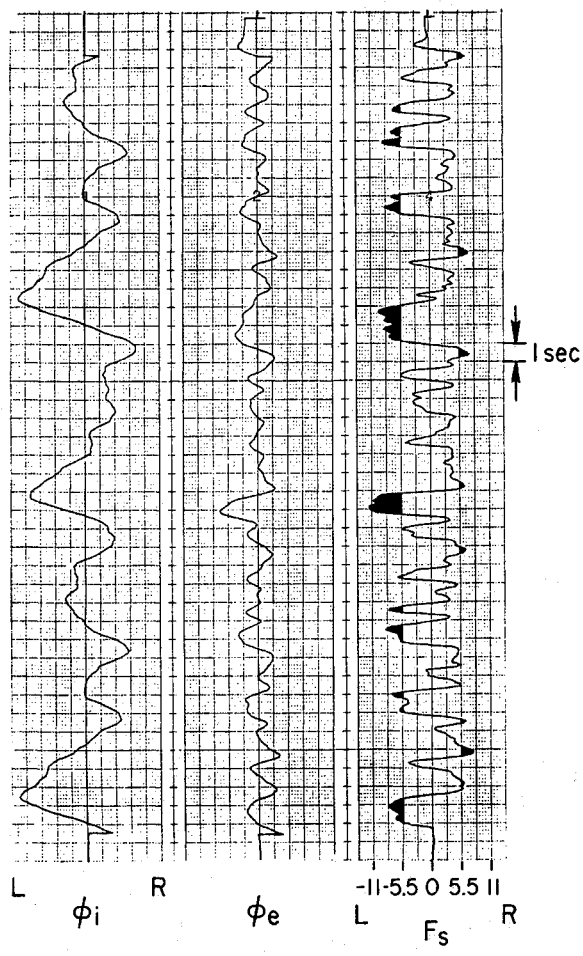

Fig. 16 Rollratchet comparison, flight and simulator.

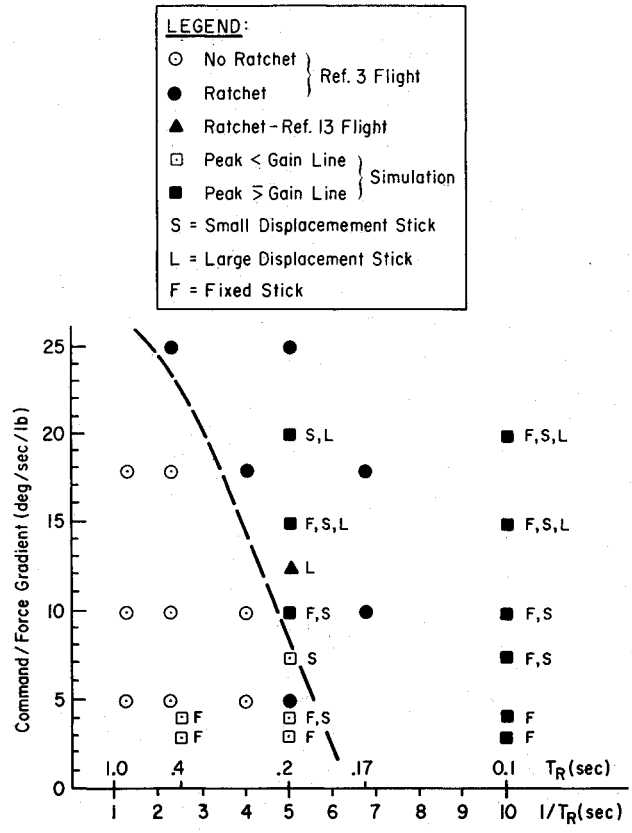

Fig. 17 Time traces of fixed force stick tracking task run 115, $K_c = 3$.

the range of time delays investigated. (It should be noted in passing that in almost every case, the ratchet only occurred with nonzero τ, as was the case in the lab simulation.) The triangular symbol at $T_R = 0.2$, $K_c = 12.5$, is another NT-33 data point obtained from a flight program in which the roll time constant was selected at 0.2 s for up-and-away tasks and 0.5 s for landing tasks.[13] In addition, two 20-rad/s first-order filters were included in the roll-rate command prefilter to "eliminate high frequency noise." Even so, this one case of ratchet tendency was observed.

The square symbols in Fig. 16 are configurations investigated in the fixed-base simulation. The open symbols identify configurations for which the Y_pY_c 0-db line did not pass through the neuromuscular peak (no ratchet possibility). The shaded squares identify configurations for which the 0-dB line passed through the peak (ratchet possibility). The letters F, S, and L reflect the displacement of the simulator side stick. It is likely that the L side stick most closely matched the NT-33 center stick characteristics.

There is very good correlation between the flight and lab simulation ratchet tendencies shown in Fig. 16. The dashed line appears to separate the nonratchet from the ratchet configurations except for the two or three lowest command/force gradient configurations at $T_R = 0.2$ s. It is possible that this difference may be related to wrist (simulation side-stick) vs arm (flight center-stick) neuromuscular subsystem contributions at the lower command (higher force) configurations. The good agreement between flight and simulator results is interpreted as an encouraging validation of the simulator definition of ratchet potential—i.e., neuromuscular peaking cut by the Y_pY_c 0-dB line.

Pilot-Manipulator System Asymmetries

It was noted in the discussion of the influence of the command/force gradient on crossover in Fig. 6 that the control bandwidth ω_c decreased markedly as the command/force gradient decreased below 4 deg/s/lb. The reason for this can be observed in the time traces of Fig. 17. The trace on the left is the random rolling motion of the target. The trace in the middle is the roll error between the target and the controlled element, the trace on the right is the stick force input to the controlled element. It will be noted on the force trace that in roll to the right, the stick force rarely exceeds 5.5 lb, but in rolls to the left the force frequently is as high as 8 lb, and shows a maximum peak at 11 lb. This is consistent with the commentary[3,12] where the pilots indicate difficulty in generating rolls to the right using the thumb but have little difficulty in rolls to the left where they can use the entire palm of their hand to generate the force. Thus, we see bimodal control in the traces of Fig. 17 with larger magnitude, shorter duration forces used in rolls to the left and lower magnitude, longer duration forces in rolls to the right. Notice that roll error average is approximately zero in the middle trace. Thus, the area under the force traces for left vs right maneuvers must be approximately the same. For right rolls, lower forces are held for longer periods of time. This results in a lower crossover or bandwidth for right rolls as compared to left rolls, and hence a lower *average* bandwidth for the run. This bimodal control characteristic was most evident for the 3 deg/s and 4 deg/s/lb controlled element or command force gradients but was also evident up as high as the 7.5 deg/s/lb; thus the reduced bandwidth shown in the Fig. 6 plots for the low gain systems. For higher command/force gradients, the forces employed in the tracking task were sufficiently low that there was little difference between left and right maneuvers.

Conclusions

This fixed-base experimental investigation has identified and quantified interactions between the pilot's neuromuscular subsystem and typical modern, high-response, roll-rate command control system mechanization aspects, including side-stick type of manipulator force/displacement configuration, command augmentation forward loop gain, controlled element effective lag-time constant, and flight control system effective time delay.

The simulation results provide insight into high-frequency roll-ratchet oscillations, low-frequency PIO, and roll-to-right control input problems previously reported in the production F-16A, NT-33 side stick, and NT-33 roll-rate command augmentation investigations. The experimental configurations encompass and/or duplicate a number of actual flight situations, and have reproduced control problems observed in flight.

Specific conclusions relating to human pilot dynamic characterizations and possible connection to roll ratchet are

Crossover Model Refinements

1) The property $\omega_c(Y_c) = \text{const}$ extends over an order of magnitude variation in K_c force gradient change. ω_c begins to fall off as very small K_c demand great pilot effort (large K_p) to keep ω_c constant.

2) Controlled element lags for $Y_c = K_c/(Ts+1)$ are almost exactly canceled by pilot lead when $T \geq 0.2$ s (lag breakpoint of 5 rad/s).

Human Pilot Limb-Manipulator Dynamics

3) The classical third-order system approximation for the limb-manipulator portion of the human neuromuscular system is both adequate and an essential minimum form needed to consider pilot-aircraft system dynamic interactions in the frequency range 8–20 rad/s.

4) The peaking tendency (damping ratio, ζ_N) of the quadratic component of the third-order approximation is a very strong function of the controlled element dynamics.

5) For all stick force/displacement characteristics investigated, the highest ζ_N (smallest peaking tendency) occurred for $Y_c = K_c/s$ controlled elements.

6) Pure time delay induces a greater peaking tendency than an equivalent time lag.

7) Distinct peaking tendencies occurred for fixed and small stick deflections for $\tau \doteq 0.07$ and 0.1 s.

8) The controlled element form that exhibited the maximum peaking tendency ($\Delta\mathcal{R} = 7$dB) was $Y_c = K_c e^{-\tau s}/s$, for $\tau = 0.067$ s. Higher and lower values of τ resulted in less peaking.

9) For large stick deflections, the peaking tendency is minimized or nonexistent.

Roll Ratchet Connections

10) The data strongly support the suggestion that the roll ratchet phenomenon is a closed-loop pilot-vehicle system interaction in which the pilot's neuromuscular dynamics play a central role.

11) The ratchet potential of a given configuration is associated with the degree of neuromuscular system peaking. This peaking tendency can be "tuned" or "detuned" by adjustments in the effective vehicle dynamics.

12) Ratchet tendencies can be detected in fixed-base tracking task simulations by careful tailoring of the forcing function, by making $Y_p Y_c$ describing function measurements over a frequency range that includes the neuromuscular system modes, and by taking into account the influence of higher-frequency motion disturbances on the pilot's effective time delay.

13) Ratchet tendencies are most severe on force-sensing side-stick manipulators with small stick deflections.

Acknowledgments

This research was conducted under Contract NAS2-11454 to the NASA Ames Research Center, Dryden Flight Research Facility. The contract technical monitor was Mr. Donald T. Berry.

References

[1]Hoh, R. H., Mitchell, D. G., Ashkenas, I. L., Klein, R. H., Heffley, R. K., Hodgkinson, J., "Proposed MIL Standard and Handbook-Flying Qualities of Air Vehicles, Vol. II: Proposed MIL Handbook," AFWAL-TR-82-3081, Nov. 1982.

[2]Harper, R. P. Jr., "In-Flight Simulation of the Lateral-Directional Handling Qualities of Entry Vehicles," Calspan Rept. TE-1243-F-2, Feb. 1961, WADC-TR-61-147.

[3]Monagan, S. J., Smith, E., and Bailey, R. E., "Lateral Flying Qualities of Highly Augmented Fighter Aircraft," AFWAL-TR-81-3171, March 1982.

[4]Smith, R. E., "Evaluation of F-18A Approach and Landing Flying Qualities Using an In-Flight Simulator," Calspan Rept. 6241-F-1, Feb. 1979.

[5]Chalk, C. R., "Excessive Roll Damping Can Cause Roll Ratchet," *Journal of Guidance, Control, and Dynamics,* Vol. 6, May-June 1983, pp. 218-219.

[6]Mitchell, D. G. and Hoh, R. H., "Flying Qualities Requirements for Roll CAS Systems," AIAA Paper 82-1356, Aug. 1982.

[7]Allen, R. W., Jex, H. R., and Magdaleno, R. E., "Manual Control Performance and Dynamic Response During Sinusoidal Vibration," AMRL-TR-73-78, Oct. 1973.

[8]Magdaleno, R. E., McRuer, D. T., and Moore, G. P., "Small Perturbation Dynamics of the Neuromuscular System in Tracking Tasks," NASA CR-1212, Dec. 1968.

[9]Magdaleno, R. E. and McRuer, D. T., "Experimental Validation and Analytical Elaboration for Models of the Pilot's Neuromuscular Subsystem in Tracking Tasks," NASA CR-1757, April 1971.

[10]McRuer, D. T. et al., "New Approaches to Human-Pilot/Vehicle Dynamic Analysis," AFFDL-TR-67-150, Feb. 1968.

[11]McRuer, D. T. and Krendel, E. S., "Mathematical Models of Human Pilot Behavior," AGARDograph 188, Jan. 1974.

[12]Garland, M. P., Nelson, M. K., and Patterson, R. C., "F-16 Flying Qualities with External Stores," AFFTC-TR-80-29, Feb. 1981.

[13]Hall, G. W. and Smith, R. E., "Flight Investigation of Fighter Side-Stick Force-Deflection Characteristics," AFFDL-TR-75-39, May 1975.

[14]Magdaleno, R. E. and McRuer, D. T., "Effects of Manipulator Restraints on Human Operator Performance," AFFDL-TR-66-72, Dec. 1966.

[15]McRuer, D. T. and Magdaleno, R. E., "Human Pilot Dynamics with Various Manipulators," AFFDL-TR-66-138, Dec. 1966.

[16]Johnston, D. E. and McRuer, D. T., "Investigation of Interactions Between Limb-Manipulator Dynamics and Effective Vehicle Roll Control Characteristics," NASA CR-3983, May 1986.

[17]Jex, H. R., Magdeleno, R. E., and Jewell, W. F., "Effects On Target Tracking of Motion Simulator Drive Logic Filters," AFAMRL-TR-80-134, Aug. 1981, pp. 40, 41.

[18]Stapleford, R. L., Peters, R. A., and Alex, F. R., "Experiments and a Model for Pilot Dynamics with Visual and Motion Inputs," NASA CR-1325, May 1969.